Steel and Composite Structures, *Vol. 22, No. 1 (2016) 45-61*
DOI: http://dx.doi.org/10.12989/scs.2016.22.1.045

Research on anti-seismic property of new end plate bolt connections - Wave web girder-column joint

Haotian Jiang*, Qingning Li, Lei Yan, Chun Han, Wei Lu and Weishan Jiang

School of Civil Engineering, Xi'an University of Architecture and Technology, Xi'an 710055, China

(*Received October 19, 2015, Revised August 17, 2016, Accepted September 10, 2016*)

Abstract. The domestic and foreign scholars conducted many studies on mechanical properties of wave web steel beam and high-strength spiral stirrups confined concrete columns. Based on the previous research work, studies were conducted on the anti-seismic property of the end plate bolt connected wave web steel beam and high-strength spiral stirrups confined concrete column nodes applied with pre-tightening force. Four full-size node test models in two groups were designed for low-cycle repeated loading quasi-static test. Through observation of the stress, distortion, failure process and failure mode of node models, analysis was made on its load-carrying capacity, deformation performance and energy dissipation capacity, and the reliability of the new node was verified. The results showed that: under action of the beam-end stiffener, the plastic hinges on the end of wave web steel beam are displaced outward and played its role of energy dissipation capacity. The study results provided reliable theoretical basis for the engineering application of the new types of nodes.

Keywords: wave web steel beam - column node; high strength bolts; quasi-static test; anti-seismic property

1. Introduction

The use of high-strength concrete in building construction can not only improve the safety of building and the durability of components, but also reduce the weight of buildings and save the building materials (Li *et al*. 2009). At the same time, the use of high-strength stirrup confined concrete effectively overcomes the brittleness of concrete and improves the strength and ductility of concrete (Kuramoto and Nishiyama 2004). Experimental studies have shown that the energy dissipation capacity and the ductility of high-strength spiral stirrup confined concrete columns are greatly improved (Nassar *et al*. 2005, Machacek and Tuma 2006, Luo and Edlund 1996), the resistance attenuation rate and magnitude of the high-strength spiral stirrup confined concrete column are slower and smaller than those of ordinary stirrup concrete column and meanwhile the constructability of structure is improved (Ibrahim *et al*. 2006). The reserved channel beam column bolt is adopted to meet the requirement of safety in structure, and can meet the advantages of convenient construction, fast construction speed and less manpower.

The wave web steel beams are formed with joining the cold-rolled wave webs and the flat flange plate through high-frequency continuous welding. Compared with the flat web, the wave web provides better supporting effects on the flange, thereby greatly improving the stability of

*Corresponding author, Ph.D., E-mail: 316195906@qq.com

http://www.techno-press.org/?journal=scs&subpage=6 ISSN: 1229-9367 (Print), 1598-6233 (Online)

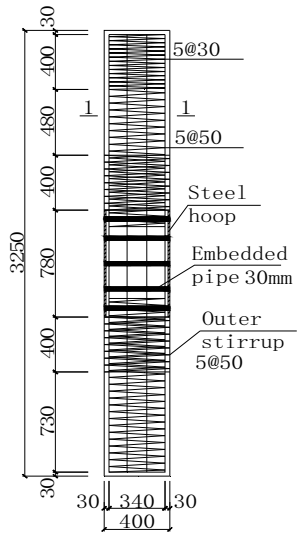

(a) Reinforcement diagram

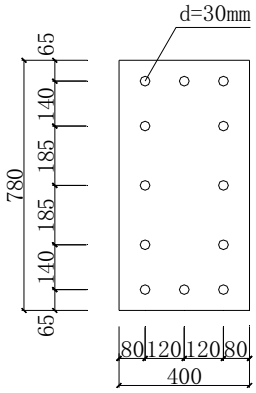

(b) Column steel plate hoop

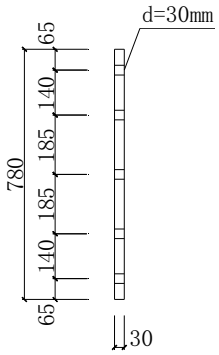

(c) Wave web size

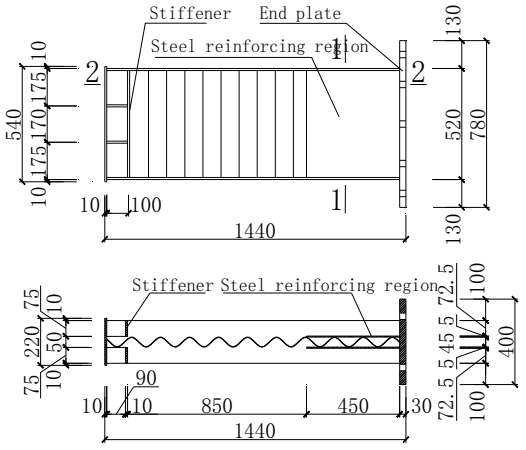

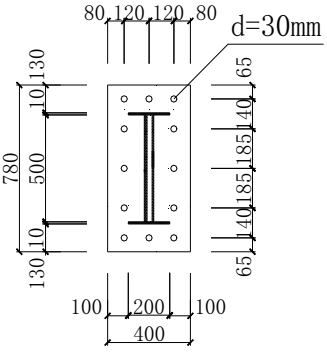

(d) Wave web steel beam size

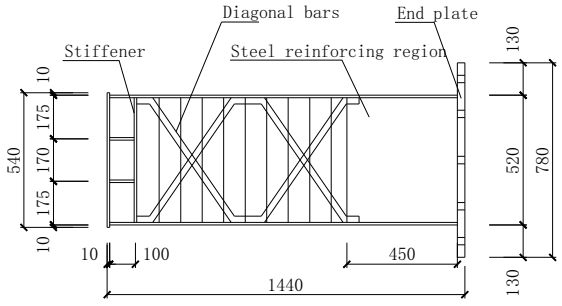

(e) Specimen PRCS-02

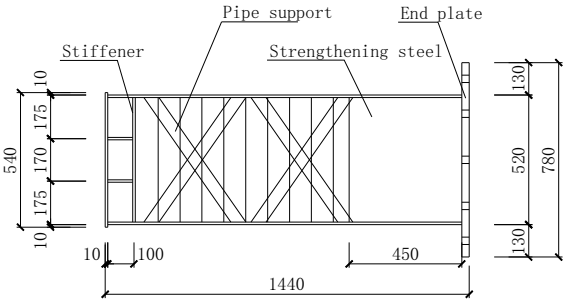

(f) Specimen PRCS-03

Fig. 1 Column Construction Detail (unit: mm)

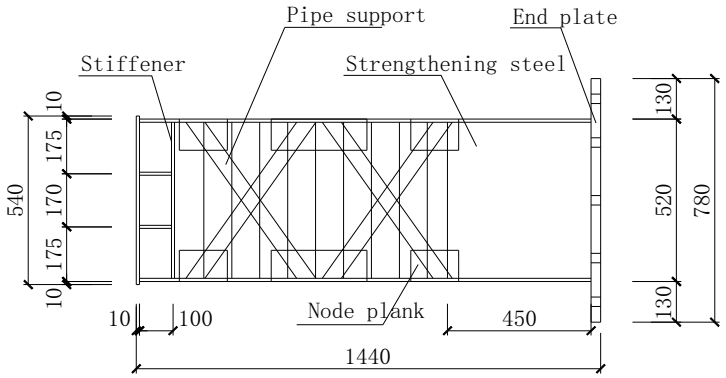

(g) Specimen PRCS-04

Fig. 1 Continued

members with the same height but much greater thickness in engineering applications, thereby reducing the quantity of structural steel. The wave web members have been widely used in many countries like the United States, Germany and Australia.

2. Test overview

2.1 Specimen design

Four full-size node models in two groups are designed in the test, numbered as PRCS-01, PRCS-02, PRCS-03, and PRCS-04 respectively, in which the specimens PRCS-02 and PRCS-04 are made by utilizing strengthening measures after the completion of tests on the specimens PRCS-01 and PRCS-03. During the assembly of specimens, pre-tightening force of 300kN is applied on the beam-column connecting bolts of the four specimens respectively, in order to ensure the rigidity and integrity of the node connection.

The section size of concrete column is 400 mm × 400 mm and the through-length of concrete column is installed with 16 pieces of C22 HRB600 longitudinal reinforcement. The four corners of the column are formed with twin bars and the stirrups utilize $A^{pw}5$ high-strength composite continuous spiral reinforcement in strength of 1,100 MPa supplied by the China Iron and Steel Institute, with the spacing of 50 mm. The stirrup densified area with the length of 400 mm is set on the top of the column, with the spacing of 30 mm.

2.2 Material performance test

C60 commodity concrete placing is utilized in the specimens, a total of nine 150 mm ×150 mm × 150mm test cubes in three groups are poured on site at the same time, maintaining 28d under the same condition as the specimen. According to the requirements in the *Standard for Test Method of Mechanical Properties on Ordinary Concrete* [GB/T50081-2002], the measured average compressive strength of the cubes is 41.9 MPa. The measured strengths of rebar and steel are as shown in Table 1.

Table 1 Mechanical property of steel

Steel grades	Diameter (thickness) /mm	Yield strength f_y/MPa	Ultimate strength f_u/MPa
A^{pw}	5	1157.51	1776.7
HRB600	22	698.3	878.3
Bolt shank	25	1026.67	1161.2
Q235	4	296.7	448.3
Q235	10	367.5	532.5

2.3 Loading Scheme [*GB/T50152-2012*]

The vertical load is first applied on the specimen in the test and then low cyclic reverse loading test is implemented on the top of the specimen, aiming at studying the reliability and the overall anti-seismic properties of the assembly nodes. The tests are carried out in the Key Laboratory of Structural Engineering and Earthquake Education Department of Xi'an University of Architecture and Technology. During the test, the vertical load is applied with 5000 kN jack and the vertical load maintains unchanged through basket-hanging pressure-stabilization device. The horizontal cyclic load is applied with 100 t actuator and the test loading apparatus is as shown in Fig. 2.

Before the test, geometry alignment is carried out for the specimen and then vertical load is is implemented on the specimen, and specimen and instrument are calibrated and then unloaded after

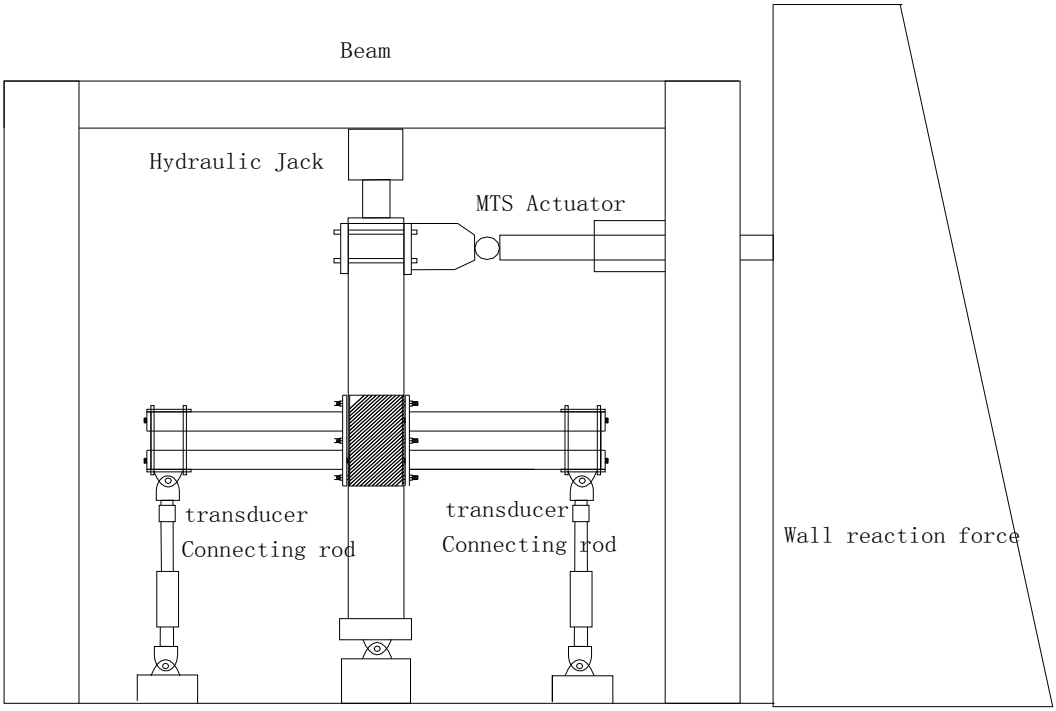

Fig. 2 Schematic for specimen loading device

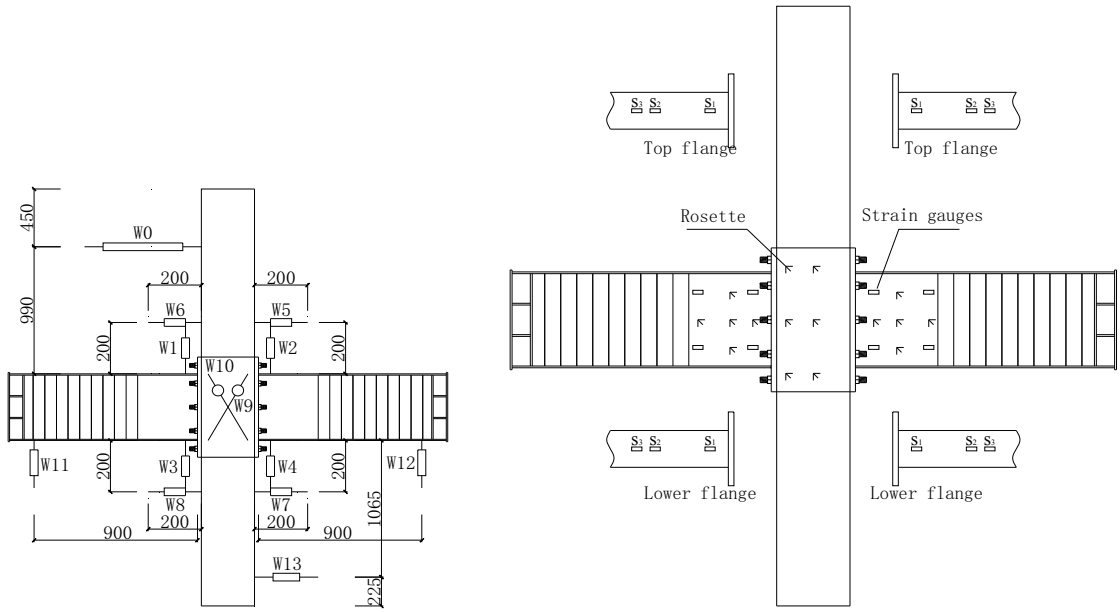

(a) Displacement meter arrangement (b) Arrangement of strain gauge and strain rosette

Fig. 3 Displacement gauge and strain gauge arrangement

the calibration. Vertical load is applied to the predetermined value once and remains unchanged through basket-hanging pressure stabilization device. Horizontal cyclic load utilizes gradation loading. The yield of specimen is judged by observing whether the tensile strain of the upper and lower flanges of the wave web steel beam has attained the yield strain. The specimen is controlled on the basis of load before the yielding and each level of load carries out recirculation once. The specimen is controlled based on displacement after the yielding and each level of displacement is 1 time the Δy (yield displacement) and each level cycles for three times. When the load drops to less than 85% of the ultimate load, the specimen is regarded as failure and loading is stopped. During the test, the continuity and uniformity of cyclic loading are always maintained and the speed of loading or unloading is kept uniform.

2.4 Measuring points layout and measurement

The displacement meter and the strain gauge are arranged as shown in Fig. 3.

3. Experimental phenomenon

To facilitate description of the test process, when the predetermined actuator is pushed eastward, the column jacking force and displacement are positive. When it is pulled westward, the column jacking force and displacement are negative. The loading orientations are as shown in Fig. 4.

(1) Loading stage with force controlled, when the specimen PRCS-01 is pushed eastward by 180.0 kN, fine cracks with the length of about 150 mm occur at 70 mm from the lower

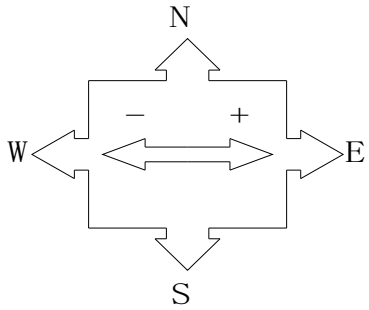

Fig. 4 Schematic for load orientations

edge of the column steel plate hoop north of the column, and on the side to the steel beams on the east. When the specimen PRCS-01 is pulled westward by 180.0 kN, clattering sound is accompanied. When the specimen is pushed eastward by 187.2 kN, and the column top displacement is 35 mm, the stress at the central axis of the flange on the side where the stiffener plate edge of the wave web steel beam was away from the node was found reaching the yield stress through numerical monitoring of the specimen strain gauge, which signifies that the wave web steel beam enters the elastic-plastic stage, the yield displacement is determined as $\Delta = 35$ mm. And the one-time yield displacement of the specimen cycles for three times in accordance with the test load system. During the process of westward pulling in the first cycle of twice the yield displacement, local buckling occurs in the middle part of the wave web nearby the east wave web steel beam close to the beam end tension-compression rod, namely at 1,100 mm from the column central axis. Buckling occurs firstly in the middle of the wave web develops to the upper and lower flanges. The concentrated force of column top is -180.1 kN before the moment of buckling and the concentrated force of column top drops to -119.3 kN after buckling of wave web. The actuator returns to zero displacement point. PRCS-01 is shown in Fig. 5.

(2) During the loading stage of the specimen PRCS-02 controlled by the force, the stepwise loading system of progressively increasing 60.0 kN for each step is used. When the specimen PRCS-02 is pushed eastward by 240.0 kN and column top displacement is 35 mm, the stress at the central axis of the flange on the side where the stiffener plate edge of the wave web steel beam was away from the node was found reaching the yield stress

(a) Specimen PRCS-01 failure diagram

(b) Partial view of specimen PRCS-01 failure

Fig. 5 Specimen PRCS-01 failure diagram

(2) through numerical monitoring of the specimen strain gauge, which signifies that the wave web steel beam enters the elastic-plastic stage, this point is determined as the yield displacement, i.e., take Δ = 35 mm. Then the test enters the displacement-controlled loading stage. During the one-time yield displacement push-pull process, the local buckling phenomenon has been aggravated wave webs on the ends of tension-compression rod on the east and west wave web steel beams, and develops to the upper and lower flanges. The folds formed by the local buckling of the east beam wave web are substantially in 45 degrees with the flanges. While the buckling folds of the west beam are located at the beam end support. And the east and west wave web steel beams appear respectively new buckling intersecting with the existing fold. The diagonal reinforcement withstanding compression force shows the phenomenon of compressed bending. In the process of double yield displacement push-pull, the wave web buckling continue to develop, which the east steel beam buckling develops to the upper flange, the wave web at the intersection of buckling folds in both directions are torn. For the compression bent diagonal reinforcement in the eastward push of the actuator, the compression turns into tension during westward pulling of the actuator, so that the compression bent diagonal reinforcement is re-straightened by tension. on the outer side of the stiffening steel plate, the wave web steel beams appear bending deformation; the welding between partial diagonal reinforcement and flange cracks, the cracking places are re-welded and the test continue. During the process of 2.5 times the yield displacement push-pull, the wave web occurs severe buckling, openings appear at the intersection of buckling folds in two directions on the east wave web steel beam, and then the phenomena of opening and closing emerge during the process of push-pull. The compression diagonal reinforcement has severe compression buckling deformation. During the process of 3 times the yield displacement push-pull, the wave web buckling continues to develop, the openings at the intersection of buckling folds in two directions on the east wave web steel beam becomes larger, and are unable to close with the process of push-pull. As the diagonal reinforcement with compression buckling has been severely deformed, so it is unable to be completely straightened when subject to tension. On the outer side of stiffening steel plate, the wave web steel beam occurs apparent bending deformation, and the welding between the diagonal reinforcement and the flange has multiple places of cracking. The actuator returns to the zero displacement point. PRCS-02 is shown in Fig. 6.

(3) The loading system with first-level load of 60.0 kN and progressively increasing load of 30.0 kN for each level is utilized from the force-controlled loading stage of the specimen PRCS-03 to the displacement-controlled period of specimen yield. When the specimen is pushed eastward by 290.0 kN and column top displacement is 38 mm, the stiffener plate edge of the wave web steel beam was away from the node was found reaching the yield stress, the yield displacement of column top is determined as Δ = 38 mm. During three-cycle of one-time yield displacement of specimens, in the first cycle, the upper flange of the east wave web steel beam at the welding connection between the tension and compression steel pipe and flange appears local deformation first. In the pushing process of the first cycle of twice yield displacement, the wave web on the tension-compression rod supports on the east wave web steel beams has the local buckling phenomenon, the inclusion angle between the buckling fold and the lower flange is over 45 degrees. And during the westward pulling, the west wave web steel beam has the local buckling phenomenon at 420 mm from the tension-compression rod supports, which develops

(a) Buckling of diagonal reinforcement

(b) Welding of diagonal reinforcement

(c) Overall failure diagram

(d) Local failure diagram

Fig. 6 Failure diagram of specimen PRCS-02

obliquely upward. The webs on the east wave web steel beams appear intersection between the new buckling fold and the existing fold, when the flanges at the welding connection between the tension and compression pipes and the flanges are severely deformed on the east and west wave web steel beam, and the deformation is in step-shaped. The north of the wave web steel beam has the phenomenon of pipe bending. The actuator returns to the zero displacement point. PRCS-03 is shown in Fig. 7.

(4) The loading system with first-level load of 50.0 kN and progressively increasing load of 50.0 kN for each level is utilized from the force-controlled loading stage of the specimen PRCS-04 to the displacement-controlled period of specimen yield. When the specimen PRCS-04 is pushed eastward by 250.0 kN and column top displacement is 40 mm, the stiffener plate edge of the wave web steel beam was away from the node was found reaching the yield stress through numerical monitoring of the specimen strain gauge, which signifies that the wave web steel beam enters the elastic-plastic stage, the yield displacement of column top is determined as $\Delta = 40$ mm. During three-cycle of one-time yield displacement of specimens, in the first cycle, some of the buckling folds of the east and west wave web steel beam continue to develop at the upper and lower flanges. In the pushing process of the first cycle of 1.5-time yield displacement, the wave webs at the intersection of buckling folds about 50 mm from the upper flange and at approximately 630 mm from the steel beam tension-compression rod end are torn on the east wave web steel plate and form into holes. A pipe has bending deformations, but in the subsequent tension process it can't be straightened like the diagonal reinforcement. The welding connection between the steel pipes on the tension-compression rod support end on the east wave web steel beams and the upper flange & gusset plate break, the breakage is re welded and the test continues. During eastward pushing of the second cycle of the twice

(a) Buckling of wave web

(b) Local deformation of flange

(c) Overall failure diagram

(d) Local failure diagram

Fig. 7 Specimen PRCS-03 failure diagram

(a) Failure diagram for specimen PRCS-04

(b) Partial failure diagram for specimen PRCS-04

Fig. 8 Failure diagram for specimen PRCS-04

yield displacement process, multiple welds between the steel pipe and flange & gusset plate are cracked, the webs of the east and west wave web steel plates have severe buckling deformation, among which the welding connection between the west steel beam wave web and the lower flange are partially torn. The actuator returns to the zero displacement point. PRCS-04 is shown in Fig. 8.

4. Test results and analysis

4.1 Hysteretic property

To facilitate the description, the directions in the present paper are specified as follows: the

east-west direction is loading direction of horizontal cyclic loading.

Figs. 9 and 10 are respectively the horizontal load - displacement hysteretic curves and skeleton curves of specimens.

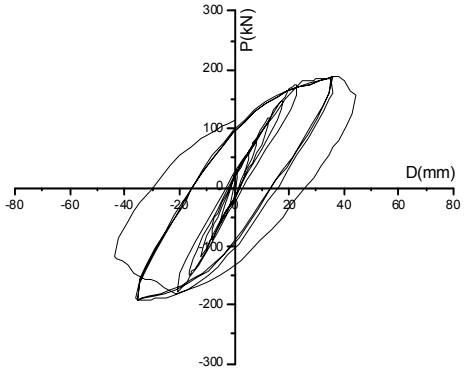

(a) PRCS-01 hysteresis curve

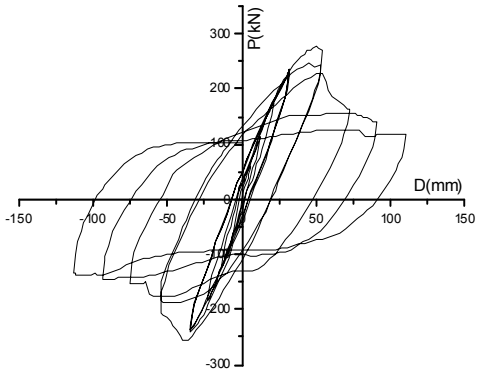

(b) PRCS-02 hysteresis curve

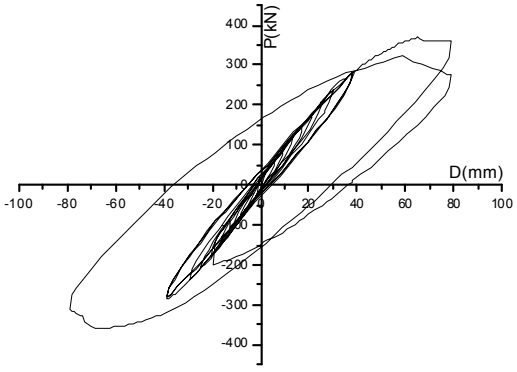

(c) PRCS-03 hysteresis curve

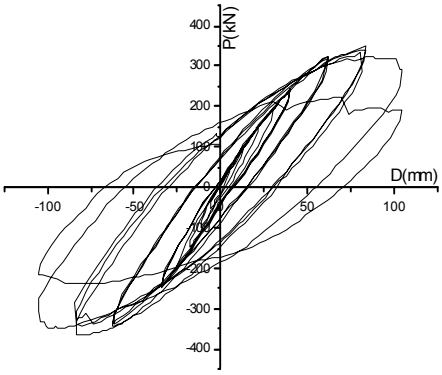

(d) PRCS-04 hysteresis curve

Fig. 9 *P*-Δ hysteresis curve of specimen

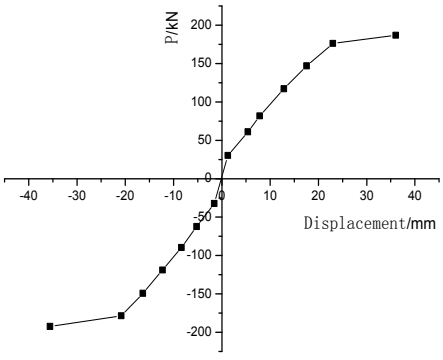

(a) PRCS-01 load-displacement skeleton curve

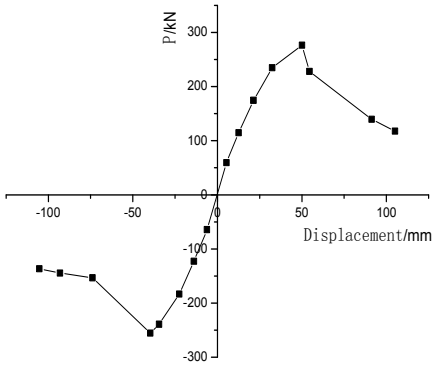

(b) PRCS-02 load-displacement skeleton curve

Fig. 10 Skeleton curve for specimen

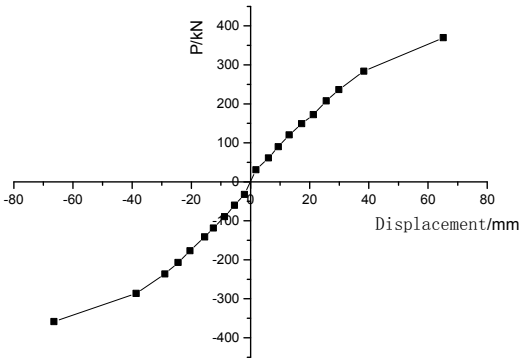

(c) PRCS-03 load-displacement skeleton curve

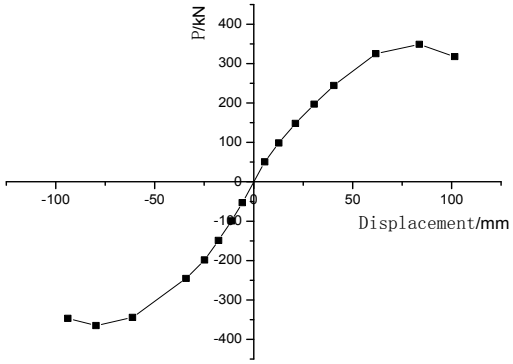

(d) PRCS-04 load-displacement skeleton curve

Fig. 10 Continued

Table 2 The characteristic points of the skeleton curve for specimen

Specimen number		Forward loading			Reverse loading		
		Peak point	Yield point	Limit point	Peak point	Yield point	Limit point
PRCS-01	Horizontal load (kN)	186.84	127.85	186.84	-192.43	-136.46	-192.43
	Horizontal displacement (mm)	36.03	14.53	36.03	-35.58	-14.65	-35.58
PRCS-02	Horizontal load (kN)	276.33	203.32	234.81	-255.52	-187.85	217.13
	Horizontal displacement (mm)	50.18	26.65	53.85	-39.72	-23.58	-52.58
PRCS-03	Horizontal load (kN)	369.57	284.92	369.57	-358.42	-277.66	-358.42
	Horizontal displacement (mm)	65.17	38.73	65.17	-66.41	-37.02	-66.41
PRCS-04	Horizontal load (kN)	348.99	250.03	348.99	-365.35	-263.21	-365.35
	Horizontal displacement (mm)	83.70	42.02	83.70	-79.66	-39.05	-79.66

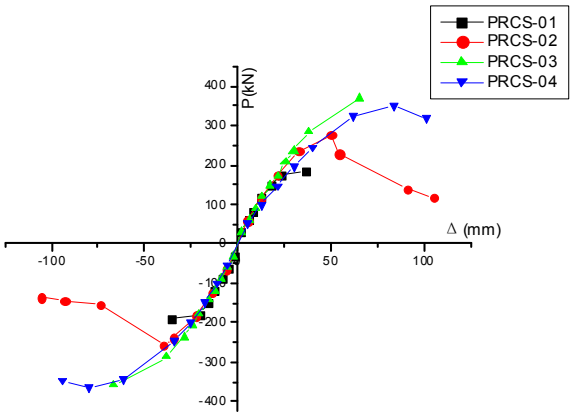

(a) Specimen skeleton curve comparison

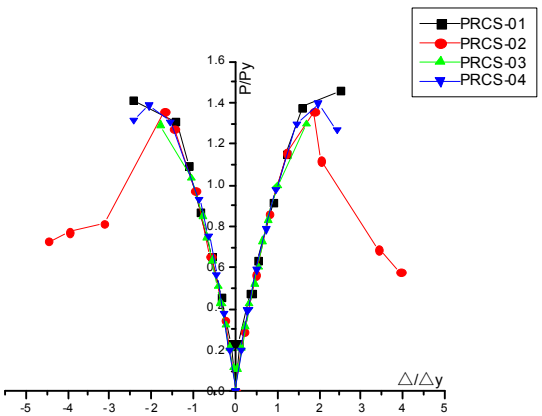

(b) Specimen dimensionless skeleton curve comparison

Fig. 11 Comparison chart between specimen skeleton curve and dimensionless skeleton curve

The skeleton curve of each specimen and dimensionless skeleton curve (P/P_y–Δ/Δ_y) are plotted in the same coordinate system, as shown in Fig. 11.

Fig. 9 shows that the hysteresis curve of the specimen is substantially in shuttle shape and free of "pinching" phenomenon. The hysteresis curves for all levels of cycle substantially coincide. It was found through comparison among hysteresis curves of the specimens that the adoption of reinforcement measures could effectively improve the energy dissipation capacity of the specimen. As seen from Fig. 10, the ultimate bearing capacities of specimens PRCS-02, PRCS-03 and PRCS-04 are significantly better than those of specimen PRCS-01. In particular, the ultimate bearing capacity of the specimen PRCS-03 is about twice as that of the specimen PRCS- 01, indicating that the test improvement program based on the principle of truss has significant effect on improving the shear capacity of wave web steel beam. As seen from comparative analysis of the skeleton curve of specimen PRCS-02 and specimen PRCS-03, steel pipes have more significant effect on improving the shear capacity of wave web steel beam than snake steel, mainly in that under condition of the same cross-sectional area, the rotation radius of hollow steel pipe is much larger than the snake steel. And compared with the steel pipe, the out-of-plane stability of the snake steel is relatively weak, the out-of-plane instability of the snake steel leads to the increase of its load-carrying capacity inferior to the steel pipe.

As can be seen from Fig. 11(a), the specimens on the four nodes have similar stiffness in the early loading period. As the load increases, the stiffness degradation rate of specimen PRCS-01 is the fastest, while the stiffness degradation rate of specimen PRCS-03 is the slowest. It can be seen that the reinforcement of steel beams can slow down the stiffness degradation to a certain extent. But through strengthening the web of steel beam, play a smaller role in the degradation of the strength of the steel beams. And the strength degradation of (2,3,4) specimen is basically the same, and the strength of the steel beam is not obvious. Through comparison in Fig. 11(b), the ultimate load of specimen PRCS-02, PRCS-03 and PRCS-04 is better than that of PRCS-01, but their yield strengths also increase correspondingly, so that the strength reserves of specimens PRCS-02, PRCS-03 and PRCS-04 are inferior to specimen PRCS-01. Generally, the four specimens did not show good ductility, mainly in that the specimens are damaged for other reasons before full development of the beam-end plastic zone.

4.2 Energy dissipation capacity (*Hasan et al.1998*)

The energy dissipation capacity of the specimens can be expressed by h_e or the energy dissipation factor E, which is a major indicator for measuring anti-seismic property of the specimen. The larger of h_e or E, the stronger energy dissipation capacity of the specimen.

The h_e and E are calculated as per Eqs. (1) and (2)

$$h_e = \frac{1}{2\pi} \cdot \frac{S_{ABCDE}}{S_{\Delta OBF} + S_{\Delta ODG}} \tag{1}$$

$$E = 2\pi h_e \tag{2}$$

In the above equations, h_e is the equivalent viscous damping coefficient, E stands for the energy dissipation coefficient, S_{ABCDE} is the area enclosed by the hysteresis loop and the displacement axis (as shown in Fig. 12) and $S_{\Delta OBF}$ and $S_{\Delta ODG}$ stand for the triangle areas enclosed by the peak point and the displacement axis.

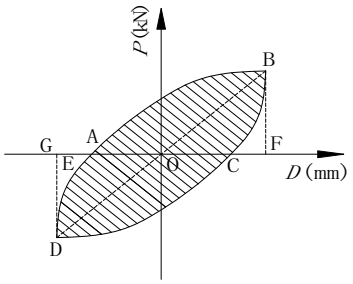

Fig. 12 Schematic diagram of hysteresis loop

Table 3 Specimens energy dissipation capacity

Specimen number	Equivalent viscous damping coefficient, h_e	Energy dissipation coefficient, E
PRCS-01	0.234	1.472
PRCS-02	0.239	1.498
PRCS-03	0.230	1.446
PRCS-04	0.267	1.677

The calculation results of equivalent viscous damping coefficient, h_e, and energy dissipation coefficient, E are shown in Table 2.

The energy dissipation capacity of the test piece PRCS-01 is better than PRCS-03, which indicates that the energy dissipation capacity of local failure of flange is not as energy dissipation capacity as the plate shear failure, so it should be avoided in the design.

The equivalent viscous damping coefficient of reinforced concrete node is generally 0.1. And the equivalent viscous damping coefficients for the four groups of nodes specimens in this experiment are more than 0.2 in average. The energy consumption of the node specimens is significantly better than that of the reinforced concrete node. If the wave web can meet the shear resistance requirements and the plastic zone of the wave web steel beam is fully developed, its energy capacity will be greater. Therefore, the end plate connecting wave web steel beam-concrete column combination nodes with reinforced beam end and applied with the bolts pretension have sufficient energy dissipation capacity to resist seismic action.

5. Stiffness degradation

Under repeated loading, as the increase of structural member concrete cracking and material plastic deformations will result in the stiffness degradation of the structural member, while the stiffness degradation is a major reason for the anti-seismic property degradation of structure. Therefore, the study on specimen stiffness degradation curve and its law becomes very necessary. In order to investigate the specimen stiffness degradation with the increased number of repeated loading under different ductility conditions, the link stiffness is introduced (Guo *et al*. 2012b, Nie *et al*. 2004), and the link stiffness K_j shall be calculated as follows

$$K_j = \sum_{i=1}^{n} P_j^i \Big/ \sum_{i=1}^{n} u_j^i \tag{3}$$

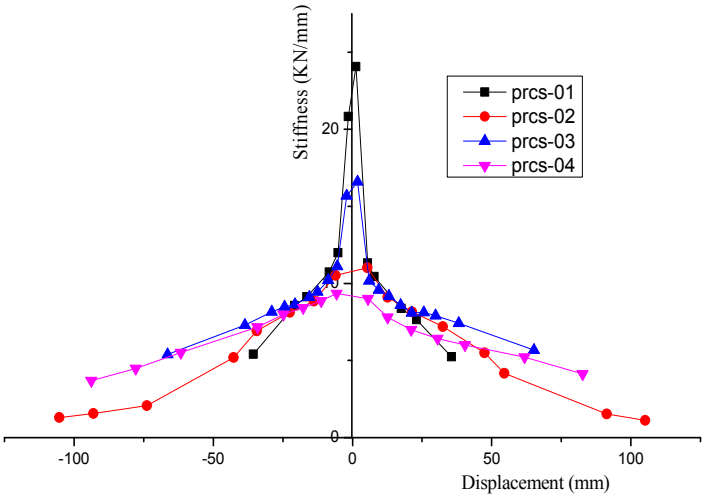

Fig. 13 Comparison chart for link stiffness degradation of each specimen

In the above equation,

K_j —stands for the cycle stiffness of the step j loading.
K_j —stands for the cycle stiffness of the step j loading.
P_j^i —stands for the load value at peak point of cycle i loading cycles at j-step loading.
u_j^i —stands for the displacement value at peak point of cycle i loading cycles at j-step loading.
n —stands for the number of cycles for displacement loading.

The link stiffness for each specimen is calculated according to the above Eq. (3), and the results are plotted in Fig. 13.

From analysis of Fig. 13, the specimens are found with similar stiffness degradation trends. In the early stage of loading, the stiffness of specimen PRCS-01 is higher than that of the specimen PRCS-03. While the only difference between the specimen PRCS-01 and the specimen PRCS-03 lies in that the specimen PRCS-03 is welded with steel pipes between the upper and lower flanges, indicating that the welding between pipe and flange affects the stiffness of the elastic phase of the specimen. From the overall stiffness degradation curve for specimen PRCS-01 and PRCS-03, the stiffness degradation for specimen PRCS-03 in various stages of loading are slower than that of specimen PRCS-01, showing that the local reinforcement of wave web of specimen using steel pipes can slow down the stiffness degradation of specimen. Through comparison of stiffness degradation curves of specimens PRCS-01,PRCS-02, PRCS-03 and PRCS-04, the stiffness degradation curves substantially coincide except that the initial stiffness varies greatly, indicating that when the specimen yields and has failure, the local reinforcement measures taken on specimen can't improve the initial stiffness of the specimen and have little effect on the specimen stiffness degradation.

6. Conclusions

Upon low-cycle repeated loading quasi-static test and study on the end plate bolt connected wave web steel beam-column nodes applied with bolt pre-tightening force, the displacement

reaction, energy consumption indicators and stiffness degradation of this new type of node are obtained, and the following conclusions are drawn:

- The wave web steel beams improves the stability of the flange plates and the local bearing capacity of webs and increases the web out-of-plane stiffness and the overall shear buckling loads due to its unique structure. The prestress of the node is pre-tightening with 300 kN, the integrity of the component is satisfied, and the stiffness of the joint is also satisfied.
- According to the experiment the yield of wave web steel beams flanges firstly appears on the outside of the steel plate in the end plate reinforcement zone, i.e., the outward transfer of plastic hinges, indicating that the outward displacement of the beam end plastic hinges by reinforcing the beam end with steel plate is feasible. According to the local reinforcement measures of the shear compression truss theory, the shear strength of the beam is significantly improved, and the bearing capacity is also increased, but the strength of the specimen is not much affected.
- Its shear elastic or bearing capacity upon elastoplastic buckling rapidly declined, and the post-buckling strength almost does not exist, so its shear capacity must be strictly ensured in the design.

Acknowledgments

The authors would like to thank the Innovation The local science and technology project of Hebei Province (Grant No. 2011188) and Xi'an University of Architecture and Technology for their generous support of this research work.

References

Abbas, H.H., Sause, R. and Driver, R.G. (2007), "Analysis of flange transverse bending of corrugated web I-girders under in-plane loads", *J. Struct. Eng.*, **133**(3), 347-355.

Calado, L., Proenca, J.M., Espinha, M. and Castiglioni, C.A. (2013), "Hysteretic behavior of dissipative welded fuses for earthquake resistant composite steel and concrete frames", *Steel Compos. Struct., Int. J.*, **14**(6), 547-569.

CECS 290 (2011), *Technical Regulations on Application of Wave Web Steel Structure*, China Planning Press, Beijing, China.

Chen, Y. (2013), "Studies on mechanical properties of steel pipe concrete flange and corrugated web I-beam", Dissertation; Yantai University, Yantai, China.

Chen, H.T., Chi, X.Q. and Yan, H. (2013), "Shear strength on wave corrugated web I-shaped plate beams", *J. Highway Transport. Res. Develop.*, **30**(5), 38-46.

Cristutiu, I.M., Nunes, D.L. and Dogariu, A.I. (2012), "Experimental study on laterally restrained steel columns with variable I cross sections", *Steel Compos. Struct., Int. J.*, **13**(3), 225-238.

Ding, Y. and Liu, X.L. (2002), Code for Design of Steel Structures (GB50017-2002); "Local stability of welded I-beam web and calculation of strength upon consideration of buckling", *J. Build. Struct.*, **23**(3), 52-59.

Dong, Y.J. (2010), "Stress mechanism analysis and economy discussion on wave web I-section beam", Dissertation; Shandong Jianzhu University, Jinan, China.

GB/T50152-2012(2012), Standard for Test Methods of Concrete Structures; China Building Industry Press, Beijing, China.

Guan, Z.L. (2011), "Studies on seismic performance of CRB550 grade reinforcement confined concrete column", Dissertation; South China University of Technology, Guangzhou, China.

Guo, Y.L., Zhang, Q.L. and Wang, X. (2010), "Design theory and experimental study on shear resistance of wave web I-section member", *China Civil Eng. J.*, **43**(10), 45-52.
Guo, Y.L., Deng, J.Z. and Jiang, Z.Q. (2012a), "Design theory and experimental study on wave web flexural member", *J. Indust. Construct. Mag. Agency*, **42**(7), 30-36.
Guo, Y.L., Liu, F. and Lan, T. (2012b), "Design principles and engineering application of wave web members", *J. Construct. Technol.*, **41**(369), 20-25.
Hasan, R., Kishi, N. and Chen, W.F. (1998), "A new nonlinear connection classification system", *J. Construct. Steel Res.*, **47**(1), 119-140.
Huang, P. (2011), "Test and mechanical properties of end-plate bolted steel-concrete composite nodes", Dissertation; Hunan University, Changsha, China.
Ibrahim, S.A., EL-Dakhakhni, W.W. and Elgaaly, M. (2006), "Fatigue of corrugated-web plate girders: Analytical study", *J. Struct. Eng.*, **132**(9), 1381-1392.
Kabiri Ataabadi, A., Ziaei-Rad, S. and Hosseini-Toudeshky, H. (2012), "Compression failure and fiber-kinking modeling of laminated composites", *Steel Compos. Struct., Int. J.*, **12**(1), 53-72.
Kuramoto, H. and Nishiyama, I. (2004), "Seismic performance and stress transferring mechanism of through-column-type joints for composite reinforced concrete and steel frames", *J. Struct. Eng.*, **130**(2), 352-360.
Li, Z.H. (2013), "Analysis on Seismic Behaviors of Steel Beam - Reinforced Concrete Column (RCS) Composite Frame Structure", Dissertation; Central South University, Changsha, China.
Li, S.C. and Huang, X.Y. (2013), "Experimental study on seismic behaviors of extended end-plate connected honeycomb steel beam - Concrete column combination node", *J. Build. Struct.*, **34**(11), 91-97.
Li, X. (2009), "Seismic behavior of bolted end-plate connections for composite steel and concrete structures", Dissertation; HuNan University, Changsha, China.
Lu, X., Yin, X. and Jiang, H. (2014), "Experimental study on Hysteretic properties of SRC columns with high steel ratio", *Steel Compos. Struct., Int. J.*, **17**(3), 287-303.
Luo, R. and Edlund, B. (1996), "Ultimate strength of girders with trapezoidally corrugated webs under patch loading", *Thin-Wall. Struct.*, **24**(2), 135-156.
Machacek, J. and Tuma, M. (2006), "Fatigue life of girders with undulating webs", *J. Construct. Steel Res.*, **62**(1), 168-177.
Men, J.J., Shi, Q.X. and Zhou, Q. (2012), "Progress of studies on reinforced concrete column - Steel beam composite frame nodes", *J. Struct. Eng.*, **28**(1), 153-157.
Meng, L. (2013), "Studies on stress properties of H-section crane beam for corrugated web", Dissertation; Hebei University of Engineering, Handan, China.
Nassar, S.A., El-Khiamy, H. and Barber, G.C. (2005), "An experimental study of bearing and thread friction in fasteners", *J. Tribol.*, **127**(2), 263-272.
Nie, J., Wang, H., Tan, Y. and Chen, G. (2004), "Experimental study on composite steel-HSC beams", *J. Build. Struct.*, **200425**(1), 58-62.
Shayanfar, M.A., Barkhordari, M.A. and Rezaeian, A.R. (2012), "Experimental study of cyclic behavior of composite vertical shear link in eccentrically braced frames", *Steel Compos. Struct., Int. J.*, **12**(1), 13-29.
Shen, H.X. and Gu, Q. (2011), "Design model of steel beam-reinforced concrete columns beam-column node", *J. Eng. Mech.*, **28**(2), 86-93.
Shi, G., Shi, Y.J. and Wang, Y.Q. (2005), "Comparison among tightening sequences for high-strength bolts connecting steel structure end plate", *J. Build. Sci. Res. Sichuan*, **31**(2), 1-3.
Shi, Q.X., Yang, K. and Bai, L.G. (2011), "Experimental study on seismic behaviors of high strength stirrup-confined high-strength concrete columns", *China Civil Eng. J.*, **44**(12), 9-17.
Theofanous, M. and Gardner, L. (2011), "Effect of element interaction and material nonlinearityon the ultimate capacity of stainless steel cross-sections", *Steel Compos. Struct., Int. J.*, **12**(1), 73-92.
Tong, J.Z. and Guo, Y.L. (2013), "Studies on design method for wave web I-section beams supporting stiffener", *J. Architect. Civil Eng.*, **30**(3), 112-119.
Wang, Y., Liu, Y. and Wang, P. (2011a), "Progress in studies on beam-column rigid connection reinforced node", *Progress Steel Build. Struct.*, **13**(2), 1-7.

Wang, Y., Yu, Y.S. and Wang, P. (2011b), "Experimental study on mechanical properties of steel frame beam end plate flange plate-type reinforced joint", *J. Eng. Mech.*, **28**(3), 177-184.
Yao, S.T. (2012), "Study on application of high strength concrete in civil engineering", Dissertation; Anhui Jianzhu University, Hefei, China.
Zhang, D.F. (2013), "Studies on the mechanical properties of composite steel pipe concrete column - Steel beam node", Dissertation; Chang'an University, Xi'an, China.
Zhang, Z., Li, G.Q. and Sun, F.F. (2011), "Studies on bending capacity performances on H-shaped steel beams of corrugated web", *J. Build. Struct.*, **32**(10), 113-118.

CC